Published in final edited form as:
Int J Hyperthermia. 2010 ; 26(7): 686–698. doi:10.3109/02656736.2010.501511.

Conformal Microwave Array (CMA) Applicators for Hyperthermia of Diffuse Chestwall Recurrence

Paul R. Stauffer, **Paolo Maccarini**, **Kavitha Arunachalam**, **Oana Craciunescu**, **Chris Diederich**, **Titania Juang**, **Francesca Rossetto**, **Jaime Schlorff**, **Andrew Milligan**, **Joe Hsu**, **Penny Sneed**, and **Zeljko Vujaskovic**

Abstract

Purpose—This article summarizes the evolution of microwave array applicators for heating large area chestwall disease as an adjuvant to external beam radiation, systemic chemotherapy, and potentially simultaneous brachytherapy.

Methods—Current devices used for thermotherapy of chestwall recurrence are reviewed. The largest conformal array applicator to date is evaluated in four studies: i) ability to conform to the torso is demonstrated with a CT scan of a torso phantom and MR scan of the conformal waterbolus component on a mastectomy patient; ii) Specific Absorption Rate (SAR) and temperature distributions are calculated with electromagnetic and thermal simulation software for a mastectomy patient; iii). SAR patterns are measured with a scanning SAR probe in liquid muscle phantom for a buried coplanar waveguide CMA; and iv) heating patterns and patient tolerance of CMA applicators are characterized in a clinical pilot study with 13 patients.

Results—CT and MR scans demonstrate excellent conformity of CMA applicators to contoured anatomy. Simulations demonstrate effective control of heating over contoured anatomy. Measurements confirm effective coverage of large treatment areas with no gaps. In 42 hyperthermia treatments, CMA applicators provided well-tolerated effective heating of up to 500cm^2 regions, achieving target temperatures of T_{min}=41.4±0.7°C, T_{90}=42.1±0.6°C, T_{ave}=42.8±0.6°C, and T_{max}=44.3±0.8°C as measured in an average of 90 points per treatment.

Summary—The CMA applicator is an effective thermal therapy device for heating large-area superficial disease such as diffuse chestwall recurrence. It is able to cover over three times the treatment area of conventional hyperthermia devices while conforming to typical body contours.

Keywords

Microwave array; conformal applicator; superficial hyperthermia; chestwall recurrence

1. Background

1.1 Clinical Problem

Breast cancer is the most prevalent form of cancer in women, with over 192,000 new cases and 40,000 deaths reported annually in the US in 2009 (1). Prognosis is highly dependent upon the location and extent of disease. Despite continued advances in detection and treatment, outcomes for locally advanced breast cancer (LABC) remain dismal with standard neoadjuvant chemotherapy. Three and five year disease free survival rates are 65% and 55% respectively (2–4). Inflammatory breast cancer has only 15% five year survival rate (2). Failure to control breast cancer at first occurrence dramatically impairs quality of life, with escalating time required for multiple followup treatment regimens and increasing chance of complications such as disfiguring ulcerations, edema, bleeding, and pain requiring narcotics long before death. Recurrence on the chestwall occurs in up to 22% of patients

following mastectomy, depending on primary size and location, and adjuvant therapy (3). For those that recur, the median survival following recurrence is just 2 years. As encouraging motivation for the current research, survival ranges from a few months to over 30 years (4), suggesting that significantly improved survival should be possible with improved therapy. To make an impact on this disease, there is an urgent need for adjuvant therapy to increase the duration of local control and improve quality of life for these patients.

Over the past two decades, numerous clinical trials(5–8), including randomized trials in breast and chestwall disease(9–12), have shown that moderate heating to 40–45°C for 60 min combined with radiation and/or chemotherapy enhances complete response rates and improves quality of life. While encouraging, these results were obtained with equipment that was not optimized for the clinical requirements. The problem remains that hyperthermia devices typically heat only small regions while chestwall disease often spreads over large portions of the torso including the anterior and lateral chestwall and proceeding down the trunk to the abdomen and eventually to the back and shoulders. Typical cases of recurrent chestwall disease are shown in Figure 1. Numerous devices have evolved over the past three decades to heat chestwall disease, including a number of conformal applicators that can heat increasingly larger portions of the torso at one time rather than apply multiple sequential treatments of smaller regions. Following a brief review of devices and techniques available to heat chestwall recurrence of breast cancer, this article focuses on a new heat applicator becoming available for addressing diffuse chestwall disease with a significantly larger treatment area and improved patient interface for more comfortable and convenient thermotherapy.

1.2 Current Devices for Heating Chestwall (CW) Disease

Methods for heating superficial tissue disease have been reviewed previously (16–19). While ultrasound (US) systems can be focused precisely to small targets at depth(13) and have shown the ability to smear uniform heating across larger regions of the body(14) even simultaneously with external beam radiotherapy (15–17), most ultrasound systems have difficulty heating contoured anatomy and tissue overlying shallow depth bone. For this reason, treatments of recurrent CW disease are most often performed with microwave sources that limit power deposition to ≤15–20 mm depth, avoiding discomfort from underlying ribs. While microwave waveguide and horn antennas have been used extensively for treating superficial disease, these bulky applicators are flat and do not conform to the skin surface over typical patient anatomy. In addition, the need for adjustment of power deposition to accommodate variable tissue type, blood perfusion and irregularly shaped disease on contoured anatomy has necessitated a move to multiple antenna systems with variable power deposition. Thus multi-element array devices such as the 15 cm square 915 MHz 4×4 planar array microwave system (Microtherm - Labthermics Technologies Inc., Urbana IL) (18) and 12 cm diameter 8 antenna array (SA-8 - BSD Medical Corp., Salt Lake City UT) (19) have been used to increase the size and adjustability of heating patterns. As applicators increase in size to treat larger areas, the need for flexibility and improved patient interface to handle multiple power connections, surface cooling, and temperature monitoring for treatment control are intensified. The largest surface heating applicators to date include the 25 aperture 915 MHz spiral microstrip array developed at Stanford University (20) and its commercial implementation as a 24 antenna microstrip spiral array (SA-24, BSD Medical Corp., Salt Lake City UT), the 434MHz flexible PCB microstrip-based Contact Flexible Microstrip Applicator (CFMA) (21–23) and the emerging dual concentric conductor (DCC) based Conformal Microwave Array (CMA) applicator (24–31) which has subsequently been expanded for use with simultaneously administered radiation from either external beam electrons or scanning HDR brachytherapy source (32–35). This later applicator is the subject

of this article. Many other superficial heating applicators are available, but most are either small area or have large physical size with a patient interface that precludes use for large contoured areas of the torso such as that shown in Figure 1.

1.3 Thermometry for Monitoring and Control of Therapy

With appropriate efforts to filter, shield, and align wires perpendicular to the electric field, thermocouples have been used successfully in electromagnetic (EM) fields(36) but are in general not recommended for microwave thermometry(37). Instead, fiberoptic probes consisting of plastic or glass fibers with non-metallic temperature sensing elements have proven more suitable since they minimize artifacts and field perturbation. Current systems provide essentially artifact-free readout of temperature even in the most intense EM fields, with an accuracy of ±0.3°C. The probes are generally inserted through plastic catheters which may be left in the tumor between treatments with good patient tolerance. Following careful multipoint temperature calibration, High Resistance Lead Thermistors exhibit very good accuracy and precision, and long term stability(38). Similar to fiberoptics, the probes have excellent immunity to electrical readout artifacts and calibration is unique to each sensor so probes are not interchangeable. Even with EMI-immune thermal sensors, careful attention to the size and location of low dielectric constant plastic catheters is required to minimize perturbation of the radiated field in tissue (39). For monitoring and control of large area heat treatments, a small number of fixed location sensors is generally inadequate to provide feedback to multiple generators for balanced heating across heterogeneous tissues. A common method to improve characterization of the temperature distribution is to cyclically scan individual sensors through catheters lying on the skin surface and/or implanted at shallow depth in the tumor target. This thermal mapping procedure provides a linear profile of temperature readings at 5–10 mm increments along each catheter, but introduces a delay in reading temperature up to a minute or more while the probe is moving between measurement positions.

While thermal dosimetry for superficial hyperthermia has generally been performed with individual sensors that sample a small number of fixed location points, there are a number of non-invasive approaches under investigation that can quantify more complete 2-D and 3-D temperature distributions. Infrared Thermography can be useful in the measurement of large surface temperature distributions, but practical considerations of the hyperthermia applicator blocking direct vision of the heated surface have restricted its usefulness primarily to dosimetry of SAR patterns in split-phantom models (40). Alternatively, 2D temperature distributions of a surface underlying a hyperthermia applicator may be obtained using a pre-configured Thermal Monitoring Sheet (TMS) fabricated as a uniformly spaced grid of non-perturbing sensors in a thin and flexible sheet. Such a surface conforming 2D array of sensors has been proposed for clinical monitoring and feedback control of multiple element array microwave applicators when the spacing of sensors corresponds to the spacing of independently controllable heat sources (31,41,42). Other technologies are currently under investigation for their potential to read volumetric temperature distributions deep in tissue. It is well known that MW antennas can be used not only for depositing energy, but also as sensitive receivers to collect temperature-dependent blackbody radiation from nearby tissue. Microwave radiometers with multiple frequency bands to interrogate different tissue volumes at depth have demonstrated usefulness in monitoring temperature profiles of tissues up to 5 cm depth (43–47) and for control of microwave hyperthermia (48–50). Potentially simpler single band radiometers have also been proposed for balancing the power levels of multiple antenna arrays during hyperthermia treatment (30,51,52). While difficulties resulting from tissue movement during scanning remain to be solved, realtime multi-slice Magnetic Resonance Thermal Imaging (MRTI) is already a practical technique for non-invasive monitoring of volumetric tissue temperature distributions as well as physiologic

changes during heat therapy (53–57). Current efforts with proton resonance frequency shift (PRFS) based MRTI have demonstrated resolutions on the order of 0.5–1°C in 1 cm^3 sensing volumes with less than 1 min scan time for non-invasive monitoring and control of thermal therapy (58–61).

While MR thermal imaging has well-established usefulness for non-invasive volumetric dosimetry of deep hyperthermia in the pelvic region, the impact of MRTI for superficial hyperthermia is unclear at this time – especially for circulating waterbolus coupled applicators located over the thoracic region which is prone to motion artifacts. For the next few years, thermometry to control clinical hyperthermia treatments with large multiple antenna arrays is likely to be accomplished with a single EMI immune sensor located under each antenna, and/or thermal mapping of sensors across the antenna array since those technologies are readily available and provide adequate feedback to control the treatment. For enhanced control of increasingly larger antenna arrays, realtime measurement of tumor temperature distributions should move towards approaches such as 2D thermal monitoring sheets or 3D characterization of subsurface temperatures with single or multiband radiometers under each independently controllable heat source. These non-invasive monitoring approaches should be implemented soon to provide tighter control of treatment temperatures and higher minimum thermal dose within diffuse superficial disease target volumes.

2. Conformal Microwave Array Applicator for Large Area Chestwall Disease

The CMA applicator is the largest superficial hyperthermia applicator reported to date. It consists of a a thin and flexible microwave antenna array, coupled with a surface conforming waterbolus containing circulated temperature controlled water for skin surface cooling and electromagnetic coupling. An elastic support structure with optional inflatable air bladders holds the entire assembly securely over contoured anatomy. The heating component is fabricated from a flexible printed circuit board (PCB) array of the basic building block element Dual Concentric Conductor (DCC) multi-fed λ/4 square slot aperture which has been characterized previously and published extensively. Following initial optimization of the radiation pattern of DCC square slot apertures by Rossetto and others (24–26,28,29,62), Maccarini et.al.(63–65) demonstrated the ability to produce similar peripherally enhanced heating patterns that extend out to the perimeter of triangular or other polygon shapes as well as square apertures. Furthermore, the microstrip feedlines that distribute power from RF connectors on one edge of the PCB were optimized to include tuning stubs at each DCC aperture feedpoint and the original open microstrip design was replaced with coplanar waveguide buried between two ground planes to reduce losses in the PCB structure and eliminate radiation into air behind the antenna array (66). These enhancements improved matching and power efficiency of the PCB slot apertures without changing the SAR distribution in tissue.

Figure 2a shows the basic feedline design of a 3 cm square DCC slot aperture fed via buried coplanar waveguide feedlines, as optimized with electromagnetic simulations (HFSS - Ansoft Corp, Pittsburg PA) using a technique that has been reported previously(63–65). The four tuning stubs match the 50 ohm co-planar waveguide transmission lines to the feed impedance of the DCC slot and provide equal phase and amplitude microwave power to the four symmetric feed points. The tuning stubs and feedlines were designed for best impedance match of the DCC apertures radiating into human chestwall tissues through a deionized waterbolus. Simulations were performed for a range of typical tissue properties and waterbolus thicknesses and the tuning stubs adjusted to best accommodate an “average” tissue load(63–65). Figure 2b shows the computer aided design (CAD) layout of a 35 aperture array of 3 cm square DCC apertures intended to fit an “L” shape CMA applicator

for heating 42 × 27 cm area of disease spreading across the upper chest and around the side under the arm to mid-back. Figure 2c shows the corresponding waterbolus coupling layer that has been optimized for uniform distribution of temperature regulated deionized water to homogenize the temperature across the face of the large array. Following optimization of the design for fit (67) and uniformity of flow distribution (68), waterbolus prototypes such as that shown in Figure 2c have been fabricated by a commercial collaborator (Bionix Development Corp., Paoli, PA). Suitable fabrics with ~2:1 elasticity have been formed into a stretchable over-garment vest with adjustable Velcro fasteners to hold the coupling bolus and PCB antenna array securely in place over contoured anatomy. Although there are plans to integrate non-invasive microwave radiometry temperature monitoring into future CMA applicators (30, 51, 69, 70), the current applicator includes an array of skin contacting catheters crossing the waterbolus under the center of each row of DCC apertures for thermal mapping of temperature sensors during treatment. CMA applicators have been fabricated in sizes ranging from 6 to 40 individually powered 2–6 cm square DCC apertures.(31, 71, 72). Custom antenna arrays can be designed rapidly using a commercial CAD program (ADS – Agilent Corp. Santa Rosa CA) and sent to a PCB manufacturer for fabrication with a 3 week turnaround. Thin water coupling boluses (6–12 mm thick) with quick connect tube fittings and internal water distribution for uniform circulation of degassed deionized water coolant as in Figure 2c can be fabricated to match the size and shape of the custom arrays.

3. Results

Over the past decade, the CMA applicator design has evolved in terms of antenna construction, waterbolus shape and internal water distribution, and outer elastic support structure. These changes have all contributed to an improved patient interface that accommodates an increasing range of size and shape disease over highly contoured anatomy without significant change in the SAR pattern of the basic DCC-based CMA applicator. The following sections briefly summarize the results of four evaluations of CMA applicator performance in terms of: 1) conformity of current CMA applicator design to contoured anatomy, 2) theoretical ability of current CMA to heat tissue uniformly over contoured anatomy, 3) SAR measurements of the most recent buried coplanar waveguide printed circuit array configuration, and 4) a clinical evaluation of heating performance of microstrip based CMA applicators in 13 chestwall recurrence patients.

3.1 Performance Evaluation of CMA Applicators - Conformity to Chestwall

The ability of CMA applicators to conform to typical patient contours was assessed in both torso shaped phantom models that could be scanned with standard computerized tomography (CT) and in an IRB approved volunteer study to assess comfort and secure fit of the recently optimized conformal waterbolus vest with serial MR imaging. Figure 3a shows an 18-element coplanar waveguide array wrapped around the chestwall region of a torso model overlying a surface conforming rectangular waterbolus (Bionix Development Corp, Paoli PA). The applicator was secured around the contoured surface with a vest shaped elastic overgarment such as that shown in Figure 3b. A CT scan of the torso model is shown in Figure 3c to demonstrate the ability of CMA applicators to conform to an appropriately contoured surface with no trapped air pockets. The thin broken white line along the top of the 9 mm thick waterbolus is the copper DCC array apertures. Figure 3d demonstrates the close conformal fit of the waterbolus vest to a mastectomy patient chestwall. In this image, the outer white region extending from sternum under the arm to the back is a 6 mm thick waterbolus separated from skin by 0.5 mm thick PVC. The air filled catheters for thermal mapping of tumor target surface temperatures are seen (black) in intimate contact with skin (black) and waterbolus (white). Results of the 10 patient study of comfort and secure fit for 90 min “treatment” interval are reported separately.

3.2 SAR and Thermal Simulations for Large Area Disease

Thermal therapy for chestwall disease is challenging due to the large and highly contoured surface areas to be treated. It typically requires multiple treatment fields with standard 100–250 cm^2 superficial hyperthermia applicators found in most hyperthermia clinics. Larger conformal applicators that can accommodate contoured anatomy are preferred. Several multiple element array applicators have been reported in the literature, but have not been characterized for heating properties over contoured anatomy. For this effort, electromagnetic (EM) and thermal simulations were performed using commercial software and 3D simulation approaches that have been described previously for EM (63,64,66) and thermal (34,35,68,73) modeling of planar applicators. EM simulations were performed with HFSS (Ansoft Corp, Pittsburg PA) for a 42×27cm L-shape CMA to assess the ability to deliver localized heating to diffuse chestwall disease that extends from the sternum over a mastectomy scar and around the side to the back. The computer model for this situation consisted of a 15 mm deep tissue target along the contoured surface of an elliptical shape muscle-equivalent phantom “torso” coupled to the DCC array with a 1cm thick deionized water bolus. The iso-SAR patterns 10 mm deep in tissue shown in Figures 4a,b demonstrate the ability of a 35-element CMA to deliver adjustable heating patterns over a large contoured surface with no unintended gaps in effective coverage <50% SAR_{max} within the array perimeter. Heating was further characterized using finite element simulation software, Comsol (Comsol Inc. Sweden) to calculate the predicted temperature distribution for the array configuration of Figure 4b. Shown in Figure 4c is the steady state temperature distribution in one cross sectional plane of the heating array for a 42°C waterbolus. Blood perfusion rates of 2 and 1 $kg/m^3/s$ were assumed inside the target and surrounding muscle tissue for the tissue properties reported in Maccarini et al. (66). The temperature distribution in Figure 4c shows thermal elevation into the hyperthermic temperature range (40–44°C) everywhere within the 15 mm deep target tissue under the perimeter of the active heating elements.

3.3 SAR Measurement of Buried Coplanar Waveguide CMA

A 3×6 element array of 3 cm square DCC apertures spaced 2 cm apart was fabricated from 3 layer liquid crystal polymer (LCP) printed circuit board material (Rogers Corp., Chandler AZ) using a novel double ground layer buried coplanar waveguide feedline structure. This rectangular DCC array uses the 3 cm square radiating slot configuration optimized previously for microstrip DCC arrays and the new feedline design of the L-shape applicator shown in Figure 2. Figure 5a shows a photo of the 17×32 cm DCC array pattern was simulated with no power applied to the four corner elements and two central elements to demonstrate the high degree of conformability to an arbitrary heating configuration. The SAR measured in the plane 1 cm deep in liquid muscle equivalent phantom is shown in Figure 5C for this power configuration. The impedance match of this new coplanar waveguide array coupled with 6 mm waterbolus to muscle equivalent phantom load was S_{11} =10–12 db as compared to 6–7 db for earlier microstrip designs. Even better matching should be achieved with the coplanar arrays coupled to chestwall tissue for which the tuning stubs were designed.

3.4 Clinical Evaluation of CMA

A clinical evaluation of heating uniformity from CMA applicators was carried out at the University of California San Francisco under an IRB approved protocol for microwave array hyperthermia combined with external beam radiation for chestwall recurrence. Thirteen patients signed an informed consent and received one or more 60 minute heat treatments using 915 MHz Conformal Microwave Array (CMA) heat applicators ranging in size from 15 to 27 aperture arrays of 3 or 4 cm square DCC apertures. The potential effective treatment area of the CMA applicators was 375 – 500 cm^2 along the contoured anatomy

surface. Most patients also received heat treatments with a 4×4 planar array microwave system (Microtherm, Labthermics Technologies Inc. Urbana IL) with approximately 13×13 cm (169 cm^2) treatment area which was the current clinical hyperthermia system for chestwall disease at the time of this investigation. For both systems, temperatures were measured with fiberoptic sensors scanned inside 3–7 catheters crossing the tissue surface as exemplified in the left panel of Figure 1, and in some patients also at 1 cm increments along an interstitial catheter that was inserted up to 14 cm at a depth of 0.5–1 cm beneath the skin. The goals of this initial clinical evaluation of CMA applicator performance were to: i) demonstrate the ability to heat increasingly larger superficial disease regions over contoured anatomy than possible with previous microwave applicators; ii) characterize uniformity of heating of the selected target region under the conformal array, aiming for therapeutic temperatures in the range of 40 – 45°C; iii) produce high thermal dose uniformly within large target regions with acceptable toxicity, demonstrating cumulative thermal doses of $CEM43T_{90} > 10$ equivalent minutes for each treatment, and $CEM43T_{90} > 100$ total for the treatment course of 8–10 treatments, using the thermal dose calculation defined by Dewey(74) and iv) document patient comfort and tolerance to CMA treatments.

Prototype CMA applicators were used for 42 hyperthermia treatments in 13 ethnically diverse female patients with chestwall recurrence, including 7 white, 2 black, 2 Hispanic-Latino, and 2 Asian-Pacific patients. For the evaluation of heating performance of the conformal applicator, tumor target was defined as the extent of visible/palpable disease that fell within the perimeter of the DCC aperture array plus a 1cm margin. For the 42 heat treatments, the mean number of measured temperature points within the target volume was 90 ± 29, ranging from 24 to 140 points. In every treatment, an attempt was made to distribute thermal mapping catheters evenly across the tissue surface and under each independently powered aperture, and to record temperatures at 1–2 cm increments along each catheter. Due to the time required for manual mapping of large contoured areas of the torso, complete thermal maps were recorded within the first 15 min of the heat treatment and 1–2 more times during the 60 min treatment. Power levels of individual apertures were balanced based on the thermal maps to produce more uniform temperatures under the array. For this evaluation of applicator heating uniformity, temperatures are generally taken from the second thermal map which is intended to represent the steady state “adjusted” heating pattern. The mean temperatures measured within the tumor target in these 42 treatments were $T_{min} = 41.4 \pm 0.7$°C, $T_{90} = 42.1 \pm 0.6$°C, $T_{ave} = 42.8 \pm 0.6$°C, and $T_{max} = 44.3 \pm 0.8$°C. The mean cumulative equivalent minutes thermal dose was $CEM43T_{90} = 23.2 \pm 19.6$ min per treatment. Figure 6a shows a typical recording of mid-treatment thermal dosimetry for a single heat treatment with large 24 element CMA. Temperatures are shown at 1 cm increments along four catheters crossing the tumor target surface under the four rows of six DCC heat apertures. A fifth sensor was thermally mapped at 1 cm increments along an implanted catheter crossing the tumor at approximately 1 cm depth under the applicator. A waterbolus temperature of 42–42.5°C was used as previous experience with both planar and conformal microwave array applicators demonstrated most balanced heating from skin surface to depths of 1–1.5 cm at this bolus temperature. This observation has subsequently been confirmed with comprehensive thermal modeling (35). Although antenna power levels were adjusted based primarily on thermally mapped surface sensors for all patients, some of the treatments had an interstitial catheter to provide 10–15 temperatures at depth in tumor for correlation of surface and deep temperatures. Figure 6b compares heating distributions obtained near mid-treatment in an interstitial catheter 5–10 mm deep in tumor target for two different heat applicators. The dashed curve represents the average interstitial temperatures obtained in four successive treatments with the Microtherm planar array applicator and the solid line data is from a treatment of the same disease with a 24 aperture conformal microwave array. The data show that in this patient, who is typical of other chestwall recurrence cases, the CMA applicator reached higher temperatures in many but not all

portions of the tumor target, most likely due to better conformal fit of the heating antennas to the contoured surface. Direct comparison of heating uniformity within the perimeter of each applicator was possible in 7 patients treated with both a conformal array and the Microtherm planar array. Table 1 compares dosimetry parameters for the best treatment obtained with the planar array and CMA applicators treating the same disease in 7 patients. Note that the number of measured points and overall treatment volume was higher for the CMA applicators than for the planar array which was limited to 13 × 13 cm effective treatment area. Overall, the CMA applicators produced similarly effective therapeutic heating of large volume disease to the desired 41.5 – 44.5°C target range, and in most cases produced higher minimum temperatures and cumulative thermal dose over much larger target areas than possible with the waveguide array.

In addition to the quantitative thermal dosimetry summarized above, the CMA applicators were evaluated in terms of two subjective criteria, including operator friendliness and comments regarding relative comfort and tolerance to treatment from all patients that were treated with both the planar array and CMA applicator. Since the CMA ranged from 1.7 to 3 times larger effective treatment area than the waveguide array, the entire disease target was generally covered with a single CMA heat treatment whereas multiple patch area treatments were required to cover the entire disease with the smaller 15 × 15 cm waveguide array. Thus thermal mapping of larger surface areas was required for each CMA treatment, with a correspondingly larger number of measurement points and time for setup and mapping. Along with placement of the outer elastic support garment to secure the applicator to patient disease, the CMA required approximately 10 min longer for each setup. For many patients, this extra setup time was more than compensated by combining multiple 60 min patch treatments into one large area CMA treatment. While the large number of independently controlled power amplifiers required increased thermal mapping activity and translation to power adjustments during treatment, in general the operator appreciated the ability to electronically adjust heating with high resolution and to accommodate patient disease on the curving surface of the torso. So in general, the CMA required increased effort on the part of the operator for the one hour treatment but saved time in multiple treatment cases, and was more responsive to control signals to adjust power for uniform heating.

The conformal applicators included a large area thin layer waterbolus preheated to 42.5°C that was wrapped over and around the target disease prior to placement of the flexible PCB microwave array. The entire multilayer assembly was covered by an elastic strap or stretch shirt to hold the applicator snugly in place over the tissue target. Comments from all 13 patients documented that they preferred the relative comfort of the snug body conforming applicator compared to the heavy and bulky planar waveguide array which had a floppy waterbolus at the same temperature but pressed hard against the skin to ensure skin contact around the periphery of the array. The net effect was that the lightweight conformal array held to the patient surface with an elastic support was notably more comfortable and tolerable for the hour long treatment than the heavy waveguide array which some patients likened to an “elephant’s foot”. In addition, the elastic fixation of applicator over the contoured surface allowed a large range of motion for the patient whereas the planar array was supported by a holding arm that was fixed in position and thus did not allow patient movement during treatment. In fact, some patients changed positions from lying down to sitting or even standing temporarily while the CMA heating progressed uninterrupted. This ability to move during hyperthermia treatment was a significant factor in the improved comfort and tolerance of patients to the hyperthermia procedure relative to the planar waveguide array applicator. Even when the heated area covered disease up to three times the maximum area treatable with the planar array, patients tolerated the treatments better and with higher overall treatment temperatures.

4. Summary

Recurrent breast cancer patients present with a wide range of size shape, and depth disease. The literature is rife with examples of how heat can be used to enhance therapeutic results of radiation and chemotherapy, but previous clinical results have been obtained with less than optimal hyperthermia equipment that often limits the quality and extent of heating, and ease of application. This has reduced enthusiasm for thermotherapy even though the results have proven useful when heating is possible. Moving forward, there are a number of devices now available to treat breast and chestwall disease and an increasing number of devices in final stages of development for accommodating a larger number of patients with difficult to heat disease. This article provides an overview of current state of the art in heat applicators and temperature measurement approaches for diffuse superficial chestwall disease, with emphasis on a device intended to treat the largest area disease extending beyond the anterior chestwall. This CMA applicator may be configured as a conformal wrap around the anterior and lateral chest, or expanded into a complete vest to treat diffuse disease extending across the torso. An evaluation of heating performance of large conformal microwave array applicators with up to 500 cm^2 treatment area is presented. First the power deposition pattern is given for a large multiaperture DCC array coupled to a homogeneous muscle tissue-equivalent load to demonstrate the high degree of control of heating within the DCC array constructed from new coplanar waveguide feedline network. Next the power deposition pattern is calculated for a typically contoured patient and superimposed on a realistic contoured anatomy as obtained from an MR scan of a single mastectomy patient. Most importantly, CMA applicator heating performance is evaluated in a small pilot study in 13 patients heated with both a 4×4 planar waveguide array and a CMA applicator. Direct quantitative comparison of thermal dosimetry is presented for 7 patients in which the same disease site was treated with matching thermal mapping and qualitative comparison of relative patient comfort and tumor coverage is given for all 13 patients. The results demonstrate similarly therapeutic heating to the intended 41.5 – 44.5°C range within the perimeter of the heat applicators for both microwave array applicators with a minor increase in minimum and average temperatures achieved with the conformal array. In addition the conformal arrays were able to treat a larger effective area over contoured regions of the anatomy that required multiple placements of the smaller planar array applicator. Overall, the prototype conformal array applicators provided well-tolerated heating within the desired range, with temperature parameters of $T_{min} = 41.4 \pm 0.7$°C, $T_{90} = 42.1 \pm 0.6$°C, $T_{ave} = 42.8 \pm 0.6$°C, and $T_{max} = 44.3 \pm 0.8$°C obtained in an average of 90 measured points per treatment. The CMA applicator appears to be an effective hyperthermia device to treat large area superficial disease such as diffuse chestwall recurrence of breast cancer.

Acknowledgments

The authors would like to acknowledge NIH support of CMA applicator development which has evolved from work on NIH Grants RO1-CA70761, R43-CA69868, R43-AR51278, R43/44-RR14940, R43/44-CA104061, and PO1-CA42745. The authors would also like to acknowledge substantial contributions to the CMA applicator design and testing from previous active collaborators including Daniel Neuman, David Bozzo, Vinicio Manfrini, Svein Jacobsen and Yngve Birkelund. In addition, the authors would like to recognize important contributions from a number of corporate collaborators, including simulation software and technical support from Dane Thompson and Ansys/Ansoft Corp., power system from Ron Johnston at Labthermics Technologies, fiberoptic thermal monitoring sheet from Celestino Gaeta at Ipitek Corp, radiometric monitoring system from Fred Sterzer at MMTC Corp, and waterbolus and patient interface developments from Bionix Development Corp.

References

1. Cancer Facts and Figures 2009–2010. American Cancer Society; 2009.

2. Kleer CG, van Golen KL, Merajver SD. Molecular biology of breast cancer metastasis. Inflammatory breast cancer: clinical syndrome and molecular determinants. Breast Cancer Res 2000;2(6):423–9. [PubMed: 11250736]
3. Donegan W, Perez-Mesa C, Watson F. A biostatistical study of local recurrent breast cancer. Surg Gynecol Obstet 1966;122(3):529–40. [PubMed: 5908662]
4. Henderson, I.; Harris, J.; Kinne, D.; Hellman, S. Cancer of the breast. In: DeVita, VJ.; Hellman, S.; Rosenberg, S., editors. Cancer: Principles and Practice of Oncology. 3. Philadelphia: JB Lippincott Co; 1989. p. 1197-249.
5. Kapp DS. Efficacy of adjuvant hyperthermia in the treatment of superficial recurrent breast cancer: confirmation and future directions. Int J Radiat Oncol Biol Phys 1996;35(5):1117–21. [PubMed: 8751423]
6. Seegenschmiedt, MH.; Fessenden, P.; Vernon, CC. Clinical Applications. Vol. 2. Berlin, New York: Springer-Verlag; 1996. Thermoradiotherapy and Thermochemotherapy.
7. Sneed, PK.; Stauffer, PR.; Li, GC. Hyperthermia. In: Leibel, SA.; Phillips, TL., editors. Textbook of Radiation Oncology. 2. Philadelphia: W B Saunders Co; 2004. p. 1569-96.
8. Dewhirst, MW.; Jones, E.; Samulski, TV.; Vujaskovic, Z.; Li, C.; Prosnitz, L. Hyperthermia. In: Kufe, D.; Pollock, R.; Weischelbaum, R.; Gansler, RBT.; Holland, J.; FRei, E., editors. Cancer Medicine. 6. Hamilton BC: Decker; 2003. p. 623-36.
9. Jones EL, Oleson JR, Prosnitz LR, Samulski TV, Vujaskovic Z, Yu D, et al. Randomized trial of hyperthermia and radiation for superficial tumors. J Clin Onc 2005;23(13):3079–85.
10. Sherar M, Liu FF, Pintilie M, Levin W, Hunt J, Hill R, et al. Relationship between thermal dose and outcome in thermoradiotherapy treatments for superficial recurrences of breast cancer: data from a phase III trial. International Journal of Radiation Oncology, Biology, Physics 1997;39(2): 371–80.
11. Vernon CC, Hand JW, Field SB, Machin D, Whaley JB, van der Zee J, et al. Radiotherapy with or without hyperthermia in the treatment of superficial localized breast cancer: Results from five randomized controlled trials. Int J Radiat Oncol Biol Phys 1996;35(4):731–44. [PubMed: 8690639]
12. Hand JW, Machin D, Vernon CC, Whaley JB. Analysis of thermal parameters obtained during phase III trials of hyperthermia as an adjunct to radiotherapy in the treatment of breast carcinoma. Int J Hyperthermia 1997 Jul-Aug;13(4):343–64. [PubMed: 9278766]
13. Hynynen K, Pomeroy O, Smith DN, Huber PE, McDannold NJ, Kettenbach J, et al. MR imaging-guided focused ultrasound surgery of fibroadenomas in the breast: a feasibility study. Radiology (USA) 2001 Apr;219(1):176–85.
14. Hynynen K, Roemer R, Anhalt D, Johnson C, Xu ZX, Swindell W, et al. A scanned, focused, multiple transducer ultrasonic system for localized hyperthermia treatments. Int J Hyperthermia 2010 Feb;26(1):1–11. [PubMed: 20100046]
15. Moros EG, Fan X, Straube WL. Experimental assessment of power and temperature penetration depth control with a dual frequency ultrasonic system. Med Phys 1999;26(5):810–17. [PubMed: 10360546]
16. Penagaricano JA, Moros E, Novak P, Yan Y, Corry P. Feasibility of concurrent treatment with the scanning ultrasound reflector linear array system (SURLAS) and the helical tomotherapy system. Int J Hyperthermia 2008 Aug;24(5):377–88. [PubMed: 18608592]
17. Novak P, Moros EG, Straube WL, Myerson RJ. SURLAS: a new clinical grade ultrasound system for sequential or concomitant thermoradiotherapy of superficial tumors: applicator description. Med Phys 2005 Jan;32(1):230–40. [PubMed: 15719974]
18. Diederich CJ, Stauffer PR. Pre-clinical evaluation of a microwave planar array applicator for superficial hyperthermia. Int J Hyperthermia 1993;9:227–46. [PubMed: 8468507]
19. Johnson JE, Neuman DG, Maccarini PF, Juang T, Stauffer PR, Turner P. Evaluation of a dual-arm Archimedean spiral array for microwave hyperthermia. Int J Hyperthermia 2006 Sep;22(6):475–90. [PubMed: 16971368]
20. Lee ER, Wilsey TR, Tarczy-Hornoch P, Kapp DS, Fessenden P, Lohrbach AW, et al. Body conformable 915 MHz microstrip array applicators for large surface area hyperthermia. IEEE Trans Biomed Eng 1992;39(5):470–83. [PubMed: 1526638]

21. Gelvich EA, Mazokhin VN. Contact flexible microstrip applicators (CFMA) in a range from microwaves up to short waves. IEEE Trans Biomed Eng 2002;49:1015–23. [PubMed: 12214873]
22. Lamaitre G, Van Dijk JDP, Gelvich EA, Wiersma J, Schneider CJ. SAR characteristics of three types of contact flexible microstrip applicators for superficial hyperthermia. Int J Hyperthermia 1996;12(2):255–69. [PubMed: 8926393]
23. Kok HP, Correia D, De Greef M, Van Stam G, Bel A, Crezee J. SAR deposition by curved CFMA-434 applicators for superfiical hyperthermia: Measurements and simulations. Int J Hyperthermia 2010;26(2):171–84. [PubMed: 20146571]
24. Rossetto F, Stauffer PR, Manfrini V, Diederich CJ, Biffi Gentili G. Effect of practical layered dielectric loads on SAR patterns from dual concentric conductor microstrip antennas. Int J Hyperthermia 1998;14(6):513–34. [PubMed: 9886660]
25. Rossetto F, Stauffer PR. Effect of complex bolus-tissue load configurations on SAR distributions from dual concentric conductor applicators. IEEE Trans Biomed Eng 1999;46(11):1310–19. [PubMed: 10582416]
26. Rossetto F, Diederich CJ, Stauffer PR. Thermal and SAR characterization of multielement dual concentric conductor microwave applicators for hyperthermia, a theoretical investigation. Med Phys 2000;27(4):745–53. [PubMed: 10798697]
27. Rossetto F, Stauffer PR. Theoretical characterization of dual concentric conductor microwave array applicators for hyperthermia at 433 MHz. Int J Hyperthermia 2001:17.
28. Stauffer PR, Leoncini M, Manfrini V, Gentili GB, Diederich CJ, Bozzo D. Dual concentric conductor radiator for microwave hyperthermia with improved field uniformity to periphery of aperture. IEICE Trans on Communicat 1995;E78-B(6):826–35.
29. Stauffer PR, Rossetto F, Leoncini M, Gentilli GB. Radiation patterns of dual concentric conductor microstrip antennas for superficial hyperthermia. IEEE Trans Biomed Eng 1998;45(5):605–13. [PubMed: 9581059]
30. Stauffer, PR.; Jacobsen, S.; Neuman, D. Microwave Array Applicator for Radiometry Controlled Superficial Hyperthermia. In: Ryan, TP., editor. Thermal Treatment of Tissue: Energy Delivery and Assessment. San Jose: Proceedings of SPIE; 2001. p. 19-29.
31. Stauffer, P.; Maccarini, P.; Juang, T.; Jacobsen, S.; Gaeta, C.; Schlorff, J., et al. Progress on Conformal Microwave Array Applicators for Heating Chestwall Disease. In: Ryan, T., editor. Proc of SPIE. Bellingham WA: SPIE Press; 2007. p. 6440OE1-13.
32. Stauffer P, Schlorff J, Taschereau R, Juang T, Neuman D, Maccarini P, et al. Combination applicator for simultaneous heat and radiation. Conf Proc IEEE Eng Med Biol Soc 2004;4:2514–7. [PubMed: 17270784]
33. Stauffer, PR.; Schlorff, JL.; Juang, T.; Neuman, DG.; Johnson, JE.; Maccarini, PF., et al., editors. SPIE BIOS 2005. San Jose: SPIE Press; 2005. Progress on system for applying simultaneous heat and brachytherapy to large-area surface disease.
34. Arunachalam, K.; Craciunescu, O.; Maccarini, P.; Schlorff, J.; Markowitz, E.; Stauffer, P., editors. Proc of SPIE. San Jose CA: SPIE Press, Bellingham WA; 2009. Progress on ThermoBrachytherapy surface applicator for superficial tissue diseases.
35. Arunachalam K, Maccarini P, Craciunescu O, Schlorff J, Stauffer P. Thermal characteristics of thermobrachytherapy surface applicators (TBSA) for treating chestwall recurrence. Phys Med Biol 2010;55(7):1949–69. [PubMed: 20224154]
36. Chan KW, Chou CK. Use of thermocouples in the intense fields of ferromagnetic implant hyperthermia. Int J Hyperthermia 1993;9(6):831–48. [PubMed: 8106824]
37. Chan KW, Chou CK, McDougall JA, Luk KH. Changes in heating patterns due to perturbations by thermometer probes at 915 and 434 MHz. Int J Hyperthermia 1988;4(4):447–56. [PubMed: 3385232]
38. Bowman R. A probe for measuring temperature in radio-frequency heated material. IEEE Trans Mic Theory Tech 1976;24:43–5.
39. Chan KW, Chou CK, McDougall JA, Luk KH. Perturbations due to the use of catheters with non-perturbing probes. Int J Hyperthermia 1988;4(6):699–702. [PubMed: 3171264]
40. Cetas TC. Practical thermometry with a thermographic camera - calibration, transmittance, and emittance measurements. Rev Sci Instrum 1978;49(2):245–54. [PubMed: 18699070]

41. Arunachalam K, Maccarini P, Juang T, Gaeta C, Stauffer PR. Performance evaluation of a conformal thermal monitoring sheet sensor array for measurement of surface temperature distributions during superficial hyperthermia treatments. Int J Hyperthermia 2008 Jun;24(4):313–25. [PubMed: 18465416]
42. Arunachalam K, Maccarini PF, Stauffer PR. A thermal monitoring sheet with low influence from adjacent waterbolus for tissue surface thermometry during clinical hyperthermia. IEEE Trans Biomed Eng 2008 Oct;55(10):2397–406. [PubMed: 18838365]
43. Bardati F, Brown VJ, Tognolatti P. Temperature reconstructions in a dielectric cylinder by multi-frequency microwave radiometry. Journal of Electronic Waves and Applications 1993;7(11): 1549–71.
44. Hand JW, Van Leeuwen GMJ, Mizushina S, Van De Kamer JB, Maruyama K, Sugiura T, et al. Monitoring of deep brain temperature in infants using multi-frequency microwave radiometry and thermal modelling. Phys Med Biol 2001;46(7):1885–903. [PubMed: 11474932]
45. Jacobsen S, Stauffer P. Multi-frequency radiometric determination of temperature profiles in a lossy homogenous phantom using a dual-mode antenna with integral water bolus. IEEE Trans Mic Theory Tech 2002;50(7):1737–46.
46. Jacobsen S, Stauffer P. Non-invasive temperature profile estimation in a lossy medium based on multi-band radiometric signals sensed by a microwave dual-purpose body-contacting antenna. Int J Hyperthermia 2002;18(2):86–103. [PubMed: 11911486]
47. Mizushina S, Shimizu T, Suzuki K, Kinomura M, Ohba H, Sugiura T. Retrieval of temperature-depth profiles in biological objects from multi-frequency microwave radiometric data. J Electromag Waves and Appl 1993;7(11):1515–48.
48. Camart JC, Despretz D, Prevost B, Sozanski JP, Chive M, Pribetich J. New 434 MHz interstitial hyperthermia system monitored by microwave radiometry: theoretical and experimental results. Int J Hyperthermia 2000;16(2):95–111. [PubMed: 10763740]
49. Fabre JJ, Chive M, Dubois L, Camart JC, Playez E, Prevost B, et al. 915 MHz microwave interstitial hyperthermia. Part I: Theoretical and experimental aspects with temperature control by multifrequency radiometry. Int J Hyperthermia 1993;9(3):433–44. [PubMed: 8515145]
50. Chive M, Plancot M, Giaux G, Prevost B. Microwave hyperthermia controlled by microwave radiometry: technical aspects and first clinical results. J Microwave Power 1984;19(4):233–41.
51. Jacobsen S, Stauffer PR, Neuman DG. Dual-mode antenna design for microwave heating and noninvasive thermometry of superficial tissue disease. IEEE Trans Biomed Eng 2000;47(11): 1500–9. [PubMed: 11077744]
52. Jacobsen S, Stauffer PR. Can we settle with single-band radiometric temperature monitoring during hyperthermia treatment of chestwall recurrence of breast cancer using a dual-mode transceiving applicator? Physics in Medicine & Biology 2007 Feb 21;52(4):911–28. [PubMed: 17264361]
53. Wyatt C, Soher B, Maccarini P, Charles HC, Stauffer P, Macfall J. Hyperthermia MRI temperature measurement: evaluation of measurement stabilisation strategies for extremity and breast tumours. Int J Hyperthermia 2009;25(6):422–33. [PubMed: 19925322]
54. Carter DL, MacFall JR, Clegg ST, Xin W, Prescott DM, Charles HC, et al. Magnetic resonance thermometry during hyperthermia for human high-grade sarcoma. International Journal of Radiation Oncology Biology Physics 1998;40(4):815–22.
55. Hynynen K, McDannold N. MRI guided and monitored focused ultrasound thermal ablation methods: a review of progress. Int J Hyperthermia 2004 Nov;20(7):725–37. [PubMed: 15675668]
56. McDannold N, Hynynen K. Quality assurance and system stability of a clinical MRI-guided focused ultrasound system: four-year experience. Med Phys 2006 Nov;33(11):4307–13. [PubMed: 17153409]
57. Samulski TV, MacFall J, Zhang Y, Grant W, Charles C. Non-invasive thermometry using magnetic resonance diffusion imaging: potential for application in hyperthermic oncology. Int J Hyperthermia 1992;8(6):819–29. [PubMed: 1479207]
58. Craciunescu O, Stauffer P, Soher B, Maccarini P, Das S, Cheng K, et al. Accuracy of real time noninvasive temperature measurements using magnetic resonance thermal imaging in patients

treated for high grade extremity soft tissue sarcomas. Med Phys 2009;36(11):4848–58. [PubMed: 19994492]

59. Gellermann J, Wlodarczyk W, Feussner A, Fahling H, Nadobny J, Hildebrandt B, et al. Methods and potentials of magnetic resonance imaging for monitoring radiofrequency hyperthermia in a hybrid system. Int J Hyperthermia 2005 Sep;21(6):497–513. [PubMed: 16147436]
60. Gellermann J, Hildebrandt B, Issels R, Ganter H, Wlodarczyk W, Budach V, et al. Noninvasive magnetic resonance thermography of soft tissue sarcomas during regional hyperthermia: correlation with response and direct thermometry. Cancer 2006 Sep 15;107(6):1373–82. [PubMed: 16902986]
61. McDannold N. Quantitative MRI-based temperature mapping based on the proton resonant frequency shift: review of validation studies. Int J Hyperthermia 2005 Sep;21(6):533–46. [PubMed: 16147438]
62. Rossetto F, Stauffer PR. Theoretical characterization of dual concentric conductor microwave applicators for hyperthermia at 433 MHz. Int J Hyperthermia 2001 May-Jun;17(3):258–70. [PubMed: 11347730]
63. Maccarini PF, Rolfsnes HO, Neuman D, Stauffer P. Optimization of a dual concentric conductor antenna for superficial hyperthermia applications. Conf Proc IEEE Eng Med Biol Soc 2004;4:2518–21. [PubMed: 17270785]
64. Maccarini, PF.; Rolfsnes, HO.; Johnson, J.; Neuman, DG.; Jacobsen, S.; Stauffer, PR., editors. Proc of SPIE. San Jose: SPIE Press; 2005. Electromagnetic optimization of dual mode antennas for radiometry controlled heating of superficial tissue.
65. Maccarini, P.; Rolfsnes, HO.; DGN; Johnson, JE.; Juang, T.; Stauffer, PR., editors. IEEE Mic Theory and Tech Society. IEEE Press; Piscataway NJ: 2005. Advances in Microwave Hyperthermia of Large Superficial Tumors.
66. Maccarini, P.; Arunachalam, K.; Martins, C.; Stauffer, P., editors. Proc of SPIE. San Jose: SPIE Press (Bellingham WA); 2009. Size reduction and radiation pattern shaping of conformal microwave array hyperthermia applicators using multi-fed DCC slot antennas.
67. Juang T, Stauffer PR, Neuman DG, Schlorff JL. Multilayer conformal applicator for microwave heating and brachytherapy treatment of superficial tissue disease. Int J Hyperthermia 2006 Nov; 22(7):527–44. [PubMed: 17079212]
68. Arunachalam K, Maccarini PF, Schlorff JL, Birkelund Y, Jacobsen S, Stauffer PR. Design of a water coupling bolus with improved flow distribution for multi-element superficial hyperthermia applicators. Int J Hyperthermia 2009 Nov;25(7):554–65. [PubMed: 19848618]
69. Jacobsen, S.; Stauffer, PR., editors. Advances in Medical, Signal and Information Processing, 2006 MEDSIP 2006 IET 3rd International Conference. 2006. Is Single Band Radiometry Adequate for Temperature Monitoring and Control of Superficial Hyperthermia Treatments?.
70. Stauffer, PR.; Jacobsen, S.; Neuman, D.; Rossetto, F., editors. IEEE Engineering in Medicine and Biology Society. Chicago: 2000. Progress Toward Radiometry Controlled Conformal Microwave Array Hyperthermia Applicator.
71. Stauffer PR. Evolving technology for thermal therapy of cancer. Int J Hyperthermia 2005 Dec; 21(8):731–44. [PubMed: 16338856]
72. Stauffer, PR.; Diederich, CJ.; Pouliot, J. Thermal therapy for cancer. In: Thomadsen, B.; Rivard, M.; Butler, W., editors. Brachytherapy Physics. 2. Joint AAPM/ABS Summer School; p. 901-32.Med Phys Monograph No 312005
73. Birkelund Y, Jacobsen S, Arunachalam K, Maccarini P, Stauffer PR. Flow patterns and heat convection in a rectangular water bolus for use in superficial hyperthermia. Phys Med Biol 2009 Jul 7;54(13):3937–53. [PubMed: 19494426]
74. Dewey WC. Arrhenius relationships from the molecule and cell to the clinic. Int J Hyperthermia 1994;10(4):457–83. [PubMed: 7963805]

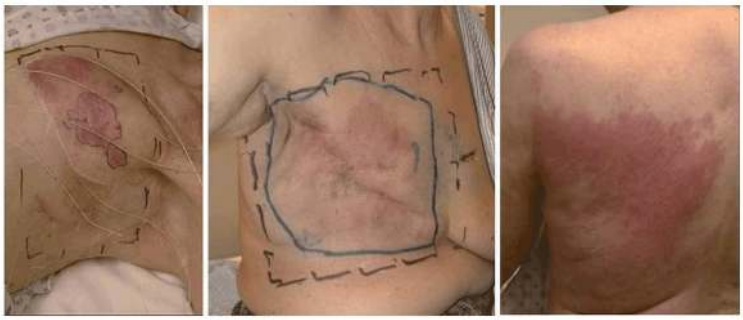

Figure 1.
Typical cases of chestwall recurrence of breast cancer to be addressed with conformal thermotherapy

Figure 2.
a) Buried coplanar waveguide feedline design to excite a single PCB square slot aperture with matching stubs on the fixed-width coplanar slot feeding each excitation port; b) matched CPW feedline distribution network to 35 element L-shaped CMA array; and c) matching 5–10 mm thick waterbolus coupling layer with optimized circulation for homogeneous temperature across large surface and integral thermal mapping catheters(34,35).

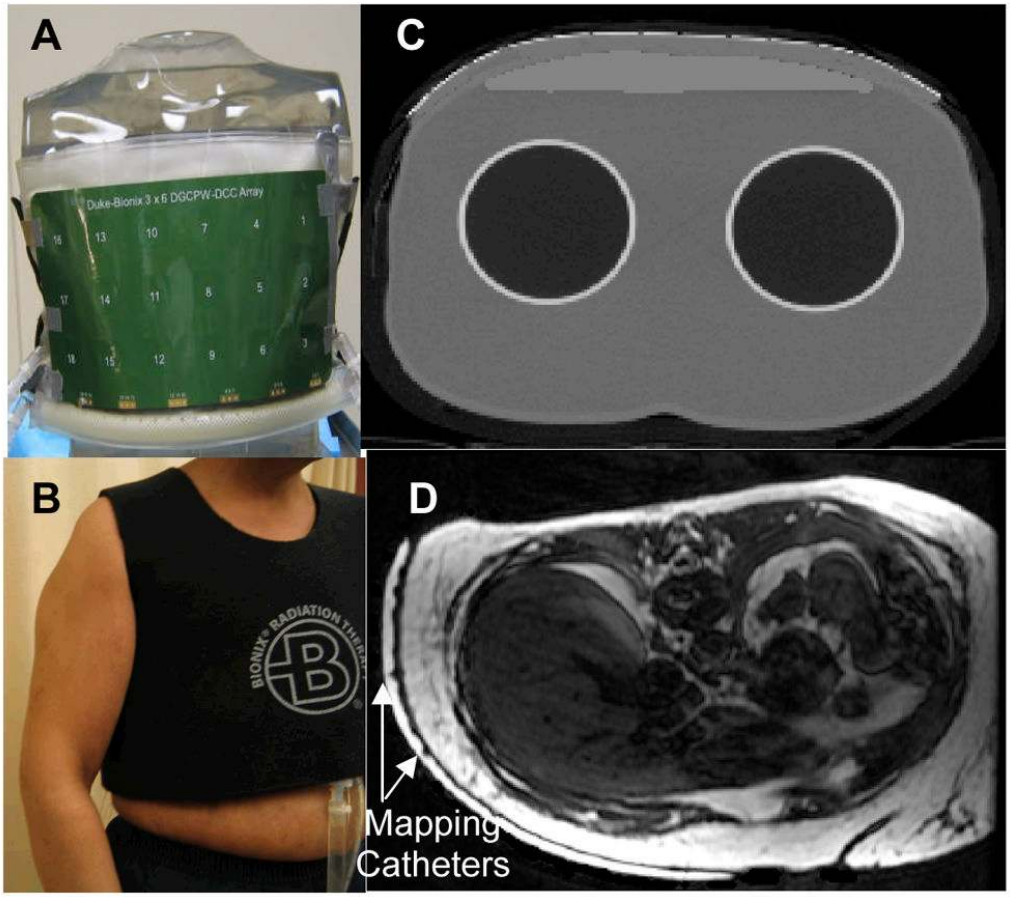

Fig 3.
CMA applicator conformity to contoured chestwall: a) Photo of 18-element DCC array coupled with 9 mm thick waterbolus to torso phantom; b) Elastic outer support vest; c) CT scan cross section of torso phantom through one row of the 18 element DCC array; d) MR scan showing conformal waterbolus on mastectomy patient.

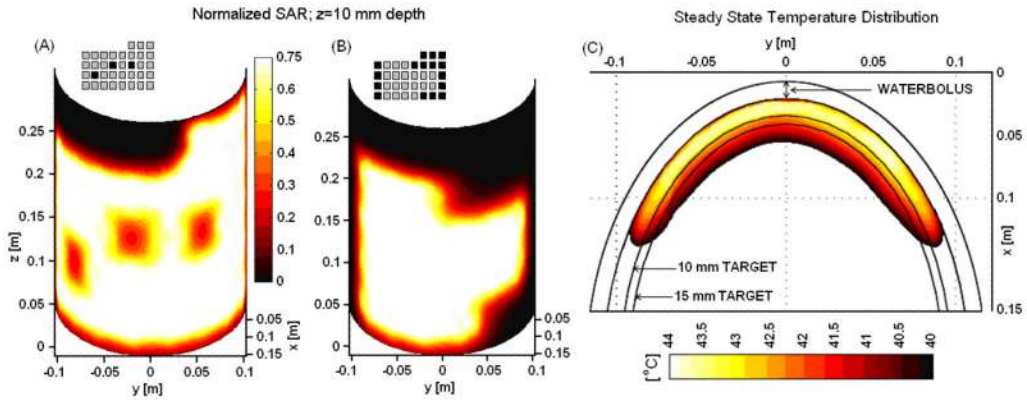

Figure 4.

Simulated SAR and heating pattern on contoured surface of an elliptical tissue model. a) Normalized SAR 10mm deep in muscle for a 35 element CMA with three centrally located DCC antennas powered off to demonstrate localization and control of heating; b) Normalized SAR pattern 10 mm deep in muscle on the contoured torso for a second power configuration as shown in inset (selected peripheral apertures in black turned off). c) Steady state temperature distribution inside the simulated target volume extending 15mm deep, as calculated for the SAR distribution of Figure 4b.

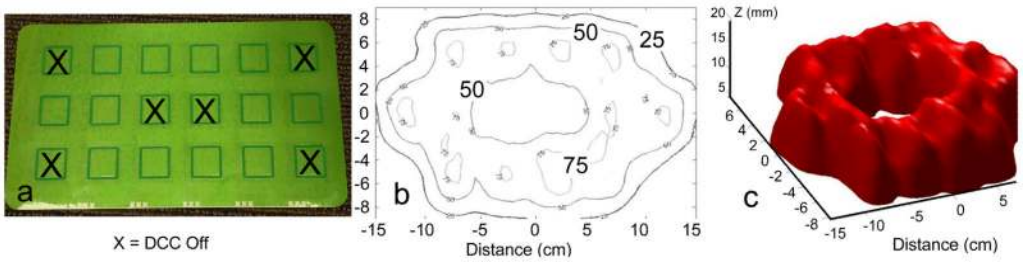

Figure 5.

a) 3×6 DCC array (17×32 cm) fabricated with three layer LCP and buried coplanar waveguide feedlines and matching stubs; b) measured SAR distribution 1 cm deep in muscle-equivalent phantom for the power configuration with antennas 1, 3, 8, 11, 16 and 18 turned off; c) 50% iso-SAR contour in the 1 cm deep plane for the power configuration shown in Figure 5a,b. Note the localization of power deposition under the DCC apertures and effective coverage of heating across large areas of tissue.

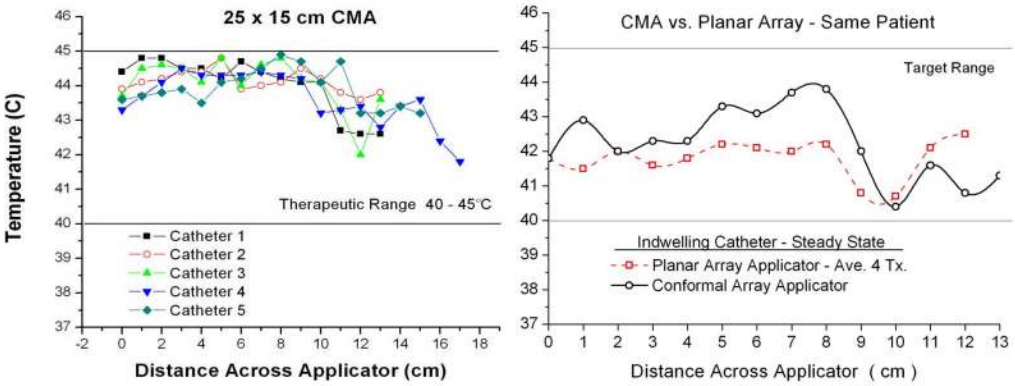

Figure 6.

Temperatures measured during clinical hyperthermia with 31 × 14 cm CMA applicator on chestwall patient. a) Temperatures measured at 1 cm increments in 4 catheters on tumor target surface and one catheter implanted approximately 1 cm deep, prior to adjusting DCC power levels for most uniform heating. b) Temperatures measured at 1 cm increments along an indwelling catheter 0.5 – 1 cm deep in tissue midway through heat treatments of the same patient, once with 24 aperture conformal array and average of four successive treatments with 16 element planar array applicator.

Table 1

Same site thermal dosimetry comparison of the best treatments with conformal microwave array (CMA) and planar array (PA) applicators. Negative values mean the planar array produced higher average temperatures for the measured points in target. Total number of measured points in tumor target is higher for CMA, proportionate to the increased treatment area. Note the planar array was limited to treating a portion (169 cm^2) of the disease target whereas the CMA coverage ranged from 288 to 500 cm^2 as needed to cover the entire tumor target.

Patient	Tmax		Tmin		T90		Tave		CEM43T90		CMA	CMA/PA
#	CMA	CMA-PA	CMA	CMA-PA	CMA	CMA-PA	CMA	CMA-PA	CMA	CMA-PA	Target	Area Ratio
1	45	1	41.1	0.4	42.2	0.1	42.3	−0.8	20	5	31 × 14	2.6
2	44.4	0.4	42.3	0.7	42.4	0.4	43	0	26	12	22 × 17	2.2
3	43.2	−1.9	41.5	0.2	42.2	0.3	42.5	−0.4	20	7	24 × 12	1.7
4	47	3.8	41.8	0.1	42.5	0.5	43	0.6	30	15	23 × 19	2.6
5	43.9	−0.1	41.3	−0.2	41.9	−0.2	42.4	−0.2	14	-3	25 × 20	3.0
6	43.2	−0.8	41.2	0.1	41.6	−0.3	42	−0.6	8	-4	25 × 20	3.0
7	44.1	0.1	42.1	0.5	42.3	0.1	43.1	0	23	14	25 × 15	2.2